

Effect of Different Exposure Conditions on the Self-healing Capacity of Engineered Cementitious Composites with Crystalline Admixture

Sina Mahmoodi ¹ and Pedram Sadeghian ²

¹ Former MASC Student, Department of Civil and Resource Engineering, Dalhousie University, 1360 Barrington Street, Halifax, NS, B3H 4R2, Canada. Email: Sina.mahmoodi@dal.ca (corresponding author)

² Associate Professor and Canada Research Chair in Sustainable Infrastructure, Department of Civil and Resource Engineering, Dalhousie University, 1360 Barrington Street, Halifax, NS, B3H 4R2, Canada. Email:

Pedram.Sadeghian@dal.ca

ABSTRACT:

In this study, the effect of different exposure conditions of ambient air, tap water, and seawater on two levels of crack widths in Engineered Cementitious Composites (ECC) were investigated. Crystalline Admixture (CA) was implemented in ECC to promote self-healing capacity. Flexural testing on prism specimens (100 mm × 100 mm × 350 mm) was conducted to evaluate the self-healing by recovering stiffness in specimens with crack widths below 200 μm. Water Permeability (WP) test was also carried out to assess the crack filling capability of ECC disk specimens (100 mm diameter × 50 mm thickness) with single crack widths over 1 mm. Digital Image Correlation (DIC) technique was used to monitor crack propagation patterns and crack widths. To analyze the microstructure of the healing products, X-ray Diffraction (XRD) test was conducted on groups of tap water and seawater exposures. Concluding results proved seawater to be a promising environmental condition for the self-healing process in ECC specimens incorporating CA, in terms of recovery of mechanical and transport properties. Brucite was found to be formed as the additional healing agent that promoted self-healing in this condition. These results can be applied for coastal concrete structures.

DOI: <http://doi.org/10.1002/suco.202200257>

KEYWORDS: ECC, Self-healing, Crystalline Admixture, Surrounding Environment, Seawater

1. INTRODUCTION

Cracks in reinforced concrete structures are inevitable due to deformation caused by hydration shrinkage, external loading, and the environmental conditions [1, 2]. The formation of cracks lowers the resistance of concrete with response to durability issues such as freezing and thawing, sulfate attacks, carbonation, and steel reinforcement corrosion [3]. Self-healing mechanisms in concrete have been investigated by researchers over the last twenty years, trying to design a mechanism capable of filling the cracks with the products coming from the concrete itself [4-8]. Autogenous self-healing mechanism is one of the main methods of self-healing and is an inherent property of concrete that existed from the first time Portland cement was used in concrete [9]. The mechanism relies on further hydration of unhydrated binders inside the cracks, and the crystallization of calcium carbonate (calcite) which is a result of the reaction between calcium ions leached from the minerals in concrete and dissolved carbonate ions in the surrounding environment [10, 11]. Nevertheless, the extend of healed cracks due to all the aforementioned contributors have been reported to be limited to about 50-150 μm and very dependable on the surrounding environment [1, 12, 13].

To improve the limitations of autogenous self-healing, the research was taken up on a special category of High-Performance Fiber Reinforced Cementitious Composites, introduced as Engineered Cementitious Composites (ECC) [14, 15]. The main characteristic of ECC that distinguishes it from other fiber-reinforced cementitious composites is its strain-hardening behavior which is the result of a synergetic interaction between fibers, cementitious matrix and the interface [16]. Regarding its self-healing properties, the dense fraction of micro-fibers limits the crack widths and helps with providing nucleation sites for healing products formation. Moreover, the high portions of fly ash in the mix that has lower hydration rate than cement, leads to greater resources of unreacted binders in the hardened concrete. These characteristics of ECC has made it a candidate for improving the autogenous self-

healing mechanism [17-20]. However, the formation of healing products is dependent on the properties of the surrounding environment such as presence of moisture, pH, temperature, and ion concentration [12, 21-24]. In particular, seawater exposure has reported promising results of autogenous self-healing in cementitious materials. While the extend of healed cracks in the presence of the moisture ranges from 50-150 μm , the healed crack width for seawater exposure is ranging between 200-700 μm [1, 12, 25, 26]. The studies on the self-healing in ECC conclude that natural environment where cycles of moisture are available, plus maintaining the cracks width below 150 μm are favorable conditions for a robust self-healing [17, 19, 20].

Crystalline Admixture is a market label used to categorize a group of hydrophilic admixtures containing active chemicals that form water-insoluble precipitates upon reaction with water, leading to densification of calcium-silicate-hydrates (C-S-H) and resisting water penetration. Active chemicals used in crystalline admixtures are types of carbonates (Na_2CO_3 , NaHCO_3 , Li_2CO_3), active silicates (sodium silicate, ethyl silicate), Talcum powder, etc. [27-30], usually mixed with crystalline promoter/catalyst, cement and sand. ACI TC212 [31] categorizes CA as type of permeability reducing admixture with the capability to function under hydrostatic pressure. The report states that tricalcium silicate (C_3S) in cement reacts with the crystalline catalyst/promoter in the presence of water to form modified CSH and pore-blocking precipitate. The carbonate ions (CO_3^{2-}) from some active chemicals can also react with calcium hydroxide ($\text{CA}(\text{OH})_2$) formed during the hydration process and produces calcite. [29, 32]. Altogether, the reactions lead to matrix densification as they fill the pores in between cement grains, minimizing drying shrinkage and ion penetration [31]. The unreacted portions of CA will be present in the matrix for late crystallization and filling the cracks when activated by moisture. The studies on the effect of CA on the self-healing properties of Fiber-Reinforced Concrete (FRC) have shown positive impacts of CA on self-healing functionality, but is still dependent on the crack

size and the surrounding environment, as almost no healing was observed in ambient air condition [33, 34]. The majority of the literature confirms that presence of water is essential for hydration or crystallization of the healing products, however, the extent of this phenomena and how different water resources can impact the self-healing capacity requires further investigation.

The current study looks into the effect of different exposure conditions of ambient air, tap water, and seawater on the self-healing of ECC containing CA through mechanical and transport properties. The purpose for the mechanical testing is to evaluate the effect of these exposure conditions on the recovery of mechanical properties of concrete in the normal range of crack formation for ECC (e.g., below 200 μm). However, the recovery of transport properties is designed to investigate the capacity of ECC containing CA to heal large cracks (>1 mm) while exposed to different exposure conditions. The significance of this work is the different crack openings considered for the experiments to evaluate the effect of CA on the recovery of mechanical and transport properties of ECC concrete exposed to different conditions. The results of this research could help understand the effect of using an improved mixture for achieving a more durable concrete, and its favorable condition.

2. EXPERIMENTAL PROGRAM

This study investigates the effect of different exposure conditions of ambient air, tap water, and seawater on the self-healing of ECC specimens containing CA through a comprehensive experimental program. Two series of prism and disk shape specimens were fabricated, pre-cracked, and then cured in the three exposure conditions. The prism specimens were used to measure the recovery of mechanical properties through a four-point bending test using the stiffness recovery ratio index. The disk specimens were fabricated to measure the crack sealing through the water permeability test. The

healing products collected from inside the cracks in the latter experiment were used for mineral determination via the X-Ray Diffraction (XRD) test. To monitor crack propagation patterns in prisms and to measure the crack opening displacement in disk specimens, Digital Image Correlation (DIC) technique was adopted in this study.

2.1. Material Properties and Specimen Fabrication

The ECC mix design adopted in this study consisted of Class-F fly ash (FA), type GU Portland cement (C), micro-silica sand (S) with an average aggregate size of 225 μm , water (W), high-range water-reducing admixture (HRWRA) and polyvinyl alcohol (PVA) fibers. Table 1. provides details on the portions of the mix design. The CA used in this study is Masterlife 300D which is a crystalline capillary waterproofing admixture product of BASF (Pinnacle Agencies Ltd., Dartmouth, NS, Canada). Based on the literature's recommendation [29, 30, 35], 2% of cement weight was selected as the CA portion in the ECC-CA mixture. Water to cementitious material ratio (W/FA+C) was 0.27. The nominal tensile strength of PVA fibers were 1100-1400 MPa, with a diameter of 38 μm , length of 8 mm and specific gravity of 1.3. The relatively high FA/C ratio of 2.2 was selected to promote the healing efficiency of ECC by late hydration [19, 36]; also, to reduce the cement portion in the mixtures.

Since moderate dispersion of PVA micro-fibers is an important issue on the final properties of ECC, a planetary mixer was used to mix ECC constituents properly. First, fly ash, cement, micro-silica sand, and CA were mixed for 2 minutes. Then, water was added gradually and after that, PVA fibers were added. Finally, the HRWRA was added, and the mixing process continued for another 1 minutes. The mixed ECC-CA was poured separately into prism molds of 100 mm \times 100 mm \times 350 mm and disk shape molds of 100 mm (diameter) \times 50 mm (thickness). After keeping the fabricated specimens under plastic sheets in a curing room with 95% relative humidity for 24 hours, the molds

were removed, and the specimens were placed back again in the humidity room up to the age of 28 days. After the moisture curing was completed, the specimens were taken out of the curing room and prepared for tests (see Figure. 1).

The seawater used in this investigation was collected from the shores of Atlantic Ocean with the ion concentrations listed in Table. 2. The containers for tap water exposure and seawater exposure were placed inside a humidity room with RH=99% and controlled temperature, so there will be no water evaporation from the containers, even though they were sealed properly. The ambient air condition for specimens was an RH of 74% and 22°C room temperature.

2.2. Test setups and plans

2.2.1. Four-point Bending

The prism specimens were pre-cracked using a four-point bending test (see Fig. 2). The test was conducted using a Universal Instron loading machine at a loading rate of 0.5mm/min and the process was monitored using DIC (Digital Image Correlation) technique. The technique allows to monitor and track points on the surface of material under displacement. For crack size measurement, the relaxation caused after unloading would also be taken into consideration by using DIC. After testing dummy specimens and monitoring DIC measurements, the required load and deflection corresponding to the desired crack size were recorded and applied to the actual samples. Multi-cracking behavior is a property of ECC in flexure, and not all the cracks are the same size, therefore in this investigation, the limit was set to be 200 μm for the maximum crack width in flexure. For each loading step, the initial stiffness was measured during the elastic region which was determined to be 10 kN for pre-cracking and 5 kN for final loading. Mid-span deflection was measured via two LVDTs placed on both sides and in the middle of the test setup. The specimen's dimensions and apparatus configuration were in accordance with ASTM C78 [37].

Upon finishing the pre-cracking stage, the specimens were placed into their exposure conditions for 6 months. After that, the prisms were removed and loaded until the failure, and the load vs. deflection of the two stages were compared. Three specimens were tested for each case, making a total number of 9 specimens

2.2.2. Water Permeability Test

To generate single-crack in disk shape specimens, a split tensile test was carried out on ECC-CA disks. As shown in Figure 3(a), rectangular wood strips were placed at the top and the bottom of the specimens to minimize the deformation effects of the loading cells on the on the interface of the disk specimens. Since obtaining identical crack widths in disk specimens was difficult (due to high volume fraction of fibers), DIC was used to measure the maximum crack width opening for each specimen, which was further used for normalizing the water permeability results. Large deflections (> 1 mm) were desired in the cracking of disk specimens to provide sufficient space inside cracks, so that the maximum capacity of self-healing in ECC-CA mix could be observed in different environments. The single crack generated in this experiment is a V-shape crack. There were also minor cracks which occurred near the single crack on the onset of crack propagation, but since the final width of the main single crack is relatively higher, the minor cracks are not considered. Water permeability test was conducted right after the cracking step and after each exposure cycle for two consecutive months. A summary of test plan for disk specimens is presented in Table. 3.

The rapid Water Permeability (WP) test for self-healing represents the amount of water passing through a crack and indicates the crack filling efficiency (sealing) over time. The literature includes different experimental methods to evaluate the self-healing of cracks by measuring the reduction in their water permeability [11, 38]. The setup built for this test is schematically shown in Figure 4 (dimensions are not to scale). It consists of three main sections, i.e., the bottom and top halves of the plastic chamber and the pipe attached from the top half. After cracking the specimens, each

was placed inside the bottom half of the fabricated plastic chamber. Then, the space between the concrete specimen and inside of the chamber was sealed using plastic rings and plumbers' putty. After that, the upper half of the chamber was placed on the bottom half, and the two halves were fixed together using six bolts. To start the test, water was poured from the top of an 8 mm tube attached to the top chamber, and the time that water traveled inside a determined 1000 mm of tube's length was measured with a stopwatch. This process was repeated three times for each specimen, and the average recorded time was used for comparison. A plastic valve was attached to the chamber to release the trapped air inside the chamber and measure the pure water pressure. The test was conducted after each month of exposure for three months, and the measured values were further used to determine the self-healing efficiency.

The WP test is intended to record and compare the travel time of water through the 1000 mm length of the tube. After initial testing, the travel time measured through the WP test was reported to vary between 3-55 seconds. The cracks generated in the specimens for this study are V-shape cracks that are not completely identical throughout their width, and the travel time depends on the free space within the cracks. Also, high fractions of PVA fibers in ECC could help with clogging the water pathway in some specimens. Therefore, to normalize the measured values, the travel time recorded (T) via the WP testing was converted into the rate of flow (Q), applying the following equation:

$$Q = \frac{V}{T} \quad \text{Eq.1}$$

where (V) is the volume of the tube in 1000mm length. To consider the effect of crack width on the recorded time, the determined value for (Q) was then used for getting velocity (U) using the following equation:

$$U = \frac{Q}{A} \quad \text{Eq.2}$$

Eq. 3 recognizes the effect of crack width through the crack area (A) perpendicular to the water travel direction. It is assumed that the area, in this case of V-shape cracks, is represented as a rectangle with a width equal to the maximum crack width generated in each specimen (W_{\max}) and a unit length. The maximum crack width was measured for specimens using the DIC technique and then used to normalize the velocity. Finally, the velocity factor (U_f) is defined as follows to be used for result comparison.

$$U_f = \frac{Q}{W_{\max}} \quad \text{Eq.3}$$

3. RESULTS AND ANALYSIS

Mechanical and transport properties were discussed in the following sections to elaborate on the efficiency of self-healing in ECC-CA exposed to different exposure conditions. Moreover, XRD analysis results provide details on the material characteristics of the healing products formed during the self-healing process.

3.1. Stiffness recovery

The recovery of stiffness in the cracked prism specimens is presented in this section to indicate the self-healing by forming healing products and providing new bonds in the cracks that could lead to recovery of mechanical properties. Fibers play an essential role in this method of recovery. They provide nucleation sites for healing product formation and connect the healing agents and the old matrix. Moreover, when fibers are enveloped by the formation of healing products, they are reinforced; therefore, their stiffness could increase. Stiffness recovery ratio (R_S) was selected in this study as the representative of recovery in mechanical properties, and is defined as follows:

$$R_S = \frac{\text{Initial stiffness of final loading}}{\text{Initial stiffness of precracking}} \leq 1 \quad \text{Eq.4}$$

The graphs represented in Fig. 5 are the load vs. mid-span displacement curves of both precracking and final loading steps. By comparing the results of the stiffness recovery ratio (R_S) for three exposure groups of ambient air, tap water and seawater, it was observed that the highest recovery ratio is for seawater condition with 78% recovery in the initial stiffness (Fig. 6). Generally, seawater proved to be a better medium for autogenous self-healing, rather than tap water with 43% or ambient air with 27% recovery. The recovery of stiffness ratio in comparison between tap water and seawater conditions suggest a 35% improvement when the submerging condition is seawater. The results show that for 200 μm cracks and fully submerged conditions, the stiffness recovery ratio of seawater condition is 1.8 times greater than tap water condition, which proves that there are other ions enhancing the self-healing reactions. Liu et al. [39] reported that the crack closure ratio of a 400 μm crack in seawater to be 2.6 times than of the same crack healed in tap water. The Presence of different ions dissolved in seawater, e.g. Mg^{2+} , helps with formation of new healing products such as brucite ($\text{Mg}(\text{OH})_2$) that can promote crack healing efficiency of ECC in addition to portlandite ($\text{CA}(\text{OH})_2$) and calcite (CaCO_3) [26]. These additional healing products can recover the stiffness of a cracked specimen through enhancing the fiber bond. When specimens are cracked up to 200 μm , healing agents are formed around the 8 mm long PVA fibers that are still connected to the matrix on both sides, and cause a higher stiffness by increasing the cross section of fibers. The mechanism for stiffness recovery is not similar to the case of compressive strength recovery. Palin et al. [40] reported that specimens healed in seawater could not recover compressive strength, however, the mechanism for the case of strength recovery is densification of concrete matrix via further hydration or carbonation, which is not as much dependent on the fibers bridging and strengthening.

3.2. Water permeability results

Fig. 7. presents the velocity factor (U_f) values obtained for each disk specimen at three-time intervals (month=0,1,2). ECC-CA specimens are categorized based on the exposure conditions, and the maximum crack width (W_{max}) for each specimen is also specified along with the specimen's ID on the charts. The authors acknowledge that comparing these values all together may not seem like a correct method of analyzing the results (due to different crack sizes and also the ambiguity of fibers orientation and dispersion inside the cracks); however, the primary goal of this experiment was to investigate the possibility of filling a large crack size in ECC specimens with CA and exposing to different environments. The reduction in the velocity factor could be taken as the capability of that particular condition to fill the cracks to some extent by reducing the water flow. Nevertheless, the results in ambient air condition indicate almost no reduction in the velocity factor over time. This result suggests that healing large cracks through hydration, carbonation, or crystallization mechanisms is not feasible without moisture [29, 30]. Even some trends in ambient air condition showed an increase in the velocity factor during the first month of exposure that could be due to the shrinkage of the cementitious composite, which subsequently increases the gap between the two faces of cracks. This behavior was more vivid during the first curing period of specimens, with an average of 74% increase in the U_f value.

As demonstrated in Fig. 7, tap water curing condition is almost neutral in terms of improvement in transport properties of ECC-CA specimens. Large deflections ($>500 \mu\text{m}$) lower the efficacy of the utilized self-healing mechanism for the formation of healing products made through binder late hydration or calcite precipitation. Even if any small healing product is formed inside the cracks, it is not impactful enough to resist the water flow. However, the results from specimens exposed to seawater prove a significant velocity reduction, especially over the first month of curing.

The average reduction for ECC-CA specimens was measured to be 77% in the first month. During the second exposure period, the trend changed to a 7-8% reduction on average. It could be concluded that due to the limited concentration of ions in the seawater used in this investigation, and the fact that seawater used in this experiment was kept unchanged throughout the experiment, most of the chemical reactions possibly took place during the first month and depleted the ions from the surrounding environment. The depletion of ions and precipitation that happened during the first month of exposure could alter the seawater pH, consequently affecting the process. The active chemicals and minerals manufactured as CA can react with ions transferred through seawater and precipitate new material. Even at large deflections and in a short period, the self-healing capability of ECC-CA exposed to seawater can be confirmed. For instance, in specimen ECC-CA7, the maximum crack width measured via DIC was 1.80mm, and it had an 82% reduction in the velocity factor over the first month.

3.3.XRD Analysis and Visual Observations

X-Ray Diffraction (XRD) test identifies the microstructure of powder samples by illuminating X-rays at them and recording its reflection. Via this test, the material characteristics of the healing products formed inside cracks in this experimental program were recognized. The test was performed on the powder samples scratched from inside the cracks of ECC-CA disk specimens. Two groups of tap water and seawater exposures were selected for this test due to their efficiency in terms of crack healing and also to determine the different healing products formed in these conditions. As shown in Fig. 9(a), the formation of new healing products took place throughout the whole crack in ECC-CA exposed to seawater, which indicates the pervasiveness of self-healing in this case. However, the visual observations proved that this formation of new products is more significant in the vicinity of the crack mouth, as it was observed to be an excess of products leaching out from the cracks in

specimen ECC-CA7 as shown in Fig. 9(b). It should be mentioned that the maximum crack width generated in this specimen was 1.80mm, and healing products were able to fill up that gap to a great extent as presented in Fig. 9(c).

To identify the observed products, XRD patterns of samples picked from ECC-CA in seawater and tap water were obtained using an X-Ray diffractometer with Cu K α radiation and 2theta ranging between 0 to 80 degrees. As results in Fig. 10 indicate, brucite (Mg(OH) $_2$) was observed in specimens submerged in seawater, which indicates the presence of Mg ions in seawater, also confirms the formation of additional healing products that enhance the autogenous healing efficiency in this exposure condition. Calcite (CaCO $_3$) was observed in both groups as a premier product of autogenous self-healing in later ages, indicating the presence of dissolved carbonate ions in tap and seawater. For seawater condition, the literature suggests the formation of aragonite (other crystal form of CaCO $_3$) rather than calcite [1, 41], however, the results show formation of calcite in seawater exposure. One contributing factor for this could be the tap water used for the water permeability test. Quartz (SiO $_2$) peaks are also determined in the samples, which could be related to the silica in the sand and FA used in ECC mixtures.

4. CONCLUSIONS

The presented experimental program measures the self-healing of ECC specimens with CA in three different exposure conditions of ambient air, tap water, and seawater. Small and large crack openings were generated in prism and disk specimens to assess the self-healing through mechanical and transport properties. From the outcomes of the tests, the following conclusion can be drawn:

- Tap water and ambient air condition were incapable of showing improvement in large crack formations. The results from water permeability test indicate that when large cracks (> 1 mm) are

present in specimens exposed to ambient air and tap water conditions, the ECC-CA is unable to fill the cracks with further hydration or calcite precipitation.

- Seawater condition proved to show the highest performance for recovery of stiffness in prism specimens, also resulted in the highest crack filling in disk specimens. The stiffness of specimens with cracks of 200 μm were recovered by 78% over a 6-month period, and maximum crack width of 1.8 mm was filled with healing products over a 2-month period. The majority of the process took place in the first month of exposure, indicating the early age improved autogenous self-healing in the marine environment.
- XRD analysis and visual observations proved the formation of additional healing products in the specimens exposed to seawater. Brucite and a mix of calcite and brucite were found to be the additional healing products formed during the curing period in seawater. Since the seawater used in this experiment was kept the same throughout the test, there is a chance that by replacing seawater at the start of each curing period, even higher self-healing levels would be observed in specimens.

The purpose of this investigation was to elaborate on the effect of different exposure conditions on the self-healing of two levels of crack openings in ECC-CA concrete. The results suggest that in seawater condition, this can be achieved. Future studies on the use and extent of self-healing mechanisms in concrete exposed to the marine environment is recommended.

ACKNOWLEDGEMENTS

This research was undertaken thanks in part to funding from the Canada First Research Excellence Fund, through the Ocean Frontier Institute. The authors would also like to appreciate the help from Subharajit Roy for co-operation in the experimental testing of the research.

REFERENCES

1. D Palin, Jonkers, HM, and Wiktor, V, *Autogenous healing of sea-water exposed mortar: Quantification through a simple and rapid permeability test*. Cement and Concrete Research, 2016. **84**: p. 1-7.
2. Peng He, Yu, Jianying, Wang, Ruiyang, Du, Wei, Han, Xiaobin, Gu, Shunjie, and Liu, Quantao, *Effect of ion chelator on pore structure, mechanical property and self-healing capability of seawater exposed mortar*. Construction and Building Materials, 2020. **246**: p. 118480.
3. Peter Taylor, Tennis, Paul, Obla, Karthik, Ram, Prashant, Van Dam, Thomas, and Dylla, Heather, *Durability of Concrete*. Transportation Research Circular, 2013(E-C171).
4. Kim Van Tittelboom and De Belie, Nele, *Self-healing in cementitious materials—A review*. Materials, 2013. **6**(6): p. 2182-2217.
5. Haoliang Huang, Ye, Guang, Qian, Chunxiang, and Schlangen, Erik, *Self-healing in cementitious materials: Materials, methods and service conditions*. Materials & Design, 2016. **92**: p. 499-511.
6. Liberato Ferrara, Van Mullem, Tim, Alonso, Maria Cruz, Antonaci, Paola, Borg, Ruben Paul, Cuenca, Estefania, Jefferson, Anthony, Ng, Pui-Lam, Peled, Alva, and Roig-Flores, Marta, *Experimental characterization of the self-healing capacity of cement based materials and its effects on the material performance: a state of the art report by COST Action SARCOS WG2*. Construction and building materials, 2018. **167**: p. 115-142.
7. Virginie Wiktor and Jonkers, Henk M, *Quantification of crack-healing in novel bacteria-based self-healing concrete*. Cement and Concrete Composites, 2011. **33**(7): p. 763-770.
8. Tae-Ho Ahn and Kishi, Toshiharu, *Crack self-healing behavior of cementitious composites incorporating various mineral admixtures*. Journal of Advanced Concrete Technology, 2010. **8**(2): p. 171-186.
9. Mario De Rooij, Van Tittelboom, Kim, De Belie, Nele, and Schlangen, Erik, *Self-healing phenomena in cement-Based materials: state-of-the-art report of RILEM technical committee 221-SHC: self-Healing phenomena in cement-Based materials*. Vol. 11. 2013: Springer.
10. Wieland Ramm and Biscopig, Michaela, *Autogenous healing and reinforcement corrosion of water-penetrated separation cracks in reinforced concrete*. Nuclear Engineering and Design, 1998. **179**(2): p. 191-200.
11. Carola Edvardsen, *Water permeability and autogenous healing of cracks in concrete*, in *Innovation in concrete structures: Design and construction*. 1999, Thomas Telford Publishing. p. 473-487.
12. Nele De Belie, Gruyaert, Elke, Al-Tabbaa, Abir, Antonaci, Paola, Baera, Cornelia, Bajare, Diana, Darquennes, Aveline, Davies, Robert, Ferrara, Liberato, and Jefferson, Tony, *A review of self-healing concrete for damage management of structures*. Advanced materials interfaces, 2018. **5**(17): p. 1800074.
13. Sina Mahmoodi and Sadeghian, Pedram. *Self-healing concrete: a review of recent research developments and existing research gaps*. in *7th International Conference on Engineering Mechanics and Materials, Laval, QC, Canada*. 2019. Canadian Society for Civil Engineering (CSCE).
14. Victor C Li, *Engineered cementitious composites (ECC)-tailored composites through micromechanical modeling*. 1998.

15. Victor C Li, *From micromechanics to structural engineering-the design of cementitious composites for civil engineering applications*. 1993.
16. Gürkan Yıldırım, Keskin, Özlem Kasap, Keskin, Süleyman Bahadır, Şahmaran, Mustafa, and Lachemi, Mohamed, *A review of intrinsic self-healing capability of engineered cementitious composites: Recovery of transport and mechanical properties*. Construction and Building Materials, 2015. **101**: p. 10-21.
17. Mustafa Sahmaran, Yildirim, Gürkan, Noori, Rezhin, Ozbay, Erdogan, and Lachemi, Mohamed, *Repeatability and pervasiveness of self-healing in engineered cementitious composites*. ACI Materials Journal, 2015. **112**(4): p. 513.
18. Gurkan Yildirim, Alyousif, Ahmed, Şahmaran, Mustafa, and Lachemi, Mohamed, *Assessing the self-healing capability of cementitious composites under increasing sustained loading*. Advances in Cement Research, 2015. **27**(10): p. 581-592.
19. Emily N Herbert and Li, Victor C, *Self-healing of microcracks in engineered cementitious composites (ECC) under a natural environment*. Materials, 2013. **6**(7): p. 2831-2845.
20. Victor C Li and Herbert, Emily, *Robust self-healing concrete for sustainable infrastructure*. Journal of Advanced Concrete Technology, 2012. **10**(6): p. 207-218.
21. Hui Ma, Qian, Shunzhi, and Zhang, Zhigang, *Effect of self-healing on water permeability and mechanical property of medium-early-strength engineered cementitious composites*. Construction and Building Materials, 2014. **68**: p. 92-101.
22. Caihong Xue, Li, Wengui, Luo, Zhiyu, Wang, Kejin, and Castel, Arnaud, *Effect of chloride ingress on self-healing recovery of smart cementitious composite incorporating crystalline admixture and MgO expansive agent*. Cement and Concrete Research. **139**: p. 106252.
23. Gürkan Yıldırım, Khiavi, Arash Hamidzadeh, Yeşilmen, Seda, and Şahmaran, Mustafa, *Self-healing performance of aged cementitious composites*. Cement and Concrete Composites, 2018. **87**: p. 172-186.
24. Sina Mahmoodi and Sadeghian, Pedram, *Self-healing of engineered cementitious composites under reversed and sustained loading conditions*. Structural Concrete.
25. Hans-Wolf Reinhardt and Jooss, Martin, *Permeability and self-healing of cracked concrete as a function of temperature and crack width*. Cement and concrete research, 2003. **33**(7): p. 981-985.
26. Muhammad Basit Ehsan Khan, Shen, Luming, and Dias-da-Costa, Daniel, *Characterisation of autogenous healing in cracked mortars under marine water exposure*. Magazine of Concrete Research, 2020: p. 1-16.
27. Xianfeng Wang, Fang, Cheng, Li, Dawang, Han, Ningxu, and Xing, Feng, *A self-healing cementitious composite with mineral admixtures and built-in carbonate*. Cement and Concrete Composites, 2018. **92**: p. 216-229.
28. Liberato Ferrara, Krelani, Visar, and Carsana, Maddalena, *A "fracture testing" based approach to assess crack healing of concrete with and without crystalline admixtures*. Construction and Building Materials, 2014. **68**: p. 535-551.
29. Marta Roig-Flores, Pirritano, F, Serna, P, and Ferrara, Liberato, *Effect of crystalline admixtures on the self-healing capability of early-age concrete studied by means of permeability and crack closing tests*. Construction and Building Materials, 2016. **114**: p. 447-457.
30. Marta Roig-Flores, Moscato, S, Serna, P, and Ferrara, Liberato, *Self-healing capability of concrete with crystalline admixtures in different environments*. Construction and Building Materials, 2015. **86**: p. 1-11.

31. ACI Committee 212, *Report on Chemical Admixtures for Concrete*. American Concrete Institute (ACI 212.3R-10), Penetron International, East Setauket, NY, USA, 2010.
32. K Sisomphon, Copuroglu, O, and Koenders, EAB, *Self-healing of surface cracks in mortars with expansive additive and crystalline additive*. *Cement and Concrete Composites*, 2012. **34**(4): p. 566-574.
33. Estefanía Cuenca, Tejedor, Antonio, and Ferrara, Liberato, *A methodology to assess crack-sealing effectiveness of crystalline admixtures under repeated cracking-healing cycles*. *Construction and Building Materials*, 2018. **179**: p. 619-632.
34. Estefanía Cuenca and Ferrara, Liberato, *Fracture toughness parameters to assess crack healing capacity of fiber reinforced concrete under repeated cracking-healing cycles*. *Theoretical and Applied Fracture Mechanics*, 2020. **106**: p. 102468.
35. Jiří Pazderka and Hájková, Eva, *Crystalline admixtures and their effect on selected properties of concrete*. *Acta Polytechnica*, 2016. **56**(4): p. 306-311.
36. Erdogan Özbay, Sahmaran, Mustafa, Yücel, Hasan E, Erdem, Tahir K, Lachemi, Mohamed, and Li, Victor C, *Effect of sustained flexural loading on self-healing of engineered cementitious composites*. *Journal of Advanced Concrete Technology*, 2013. **11**(5): p. 167-179.
37. ASTM C78 / C78M-18, *Standard Test Method for Flexural Strength of Concrete (Using Simple Beam with Third-Point Loading)*. ASTM International, West Conshohocken, PA, USA, 2018.
38. Tim Van Mullem, Gruyaert, Elke, Debbaut, Brenda, Caspeepe, Robby, and De Belie, Nele, *Novel active crack width control technique to reduce the variation on water permeability results for self-healing concrete*. *Construction and Building Materials*, 2019. **203**: p. 541-551.
39. Hao Liu, Huang, Haoliang, Wu, Xintong, Peng, Huixin, Li, Zhaoheng, Hu, Jie, and Yu, Qijun, *Effects of external multi-ions and wet-dry cycles in a marine environment on autogenous self-healing of cracks in cement paste*. *Cement and Concrete Research*, 2019. **120**: p. 198-206.
40. DAMIAN Palin, Wiktor, VIRGINIE, and Jonkers, HM, *Autogenous healing of marine exposed concrete: Characterization and quantification through visual crack closure*. *Cement and Concrete Research*, 2015. **73**: p. 17-24.
41. RA Berner, *The role of magnesium in the crystal growth of calcite and aragonite from sea water*. *Geochimica et Cosmochimica Acta*, 1975. **39**(4): p. 489-504.

Table. 1. Mix design (for 1 m³)

Mix ID	Amount (kg/m³)						
	FA	C	S	W	PVA	HRWRA	CA
ECC-CA	823	375	435	318	26	3	7.5

Table. 2. Concentration of major constituents in sea water based on the salinity of the collected area

	At salinity 30%					
	Na^+	K^+	Mg^{2+}	Ca^{2+}	Cl^-	HCO_3^-
Weight (g/kg)	9.24	0.34	1.10	0.35	16.58	0.11

Table 3. ECC-CA disk specimens test plan and exposure conditions


Cracking disk specimens with split tensile test	1 st month exposure		2 nd month exposure		
	WP test	Ambient air	WP test	Ambient air	WP test
		Tap water		Tap water	
		Seawater		Seawater	
Note: Three specimens were tested for each case, making a total number of 9 specimens.					



Fig. 1. Specimen fabricated for testing, a) prism specimens and, b) disk shape specimens

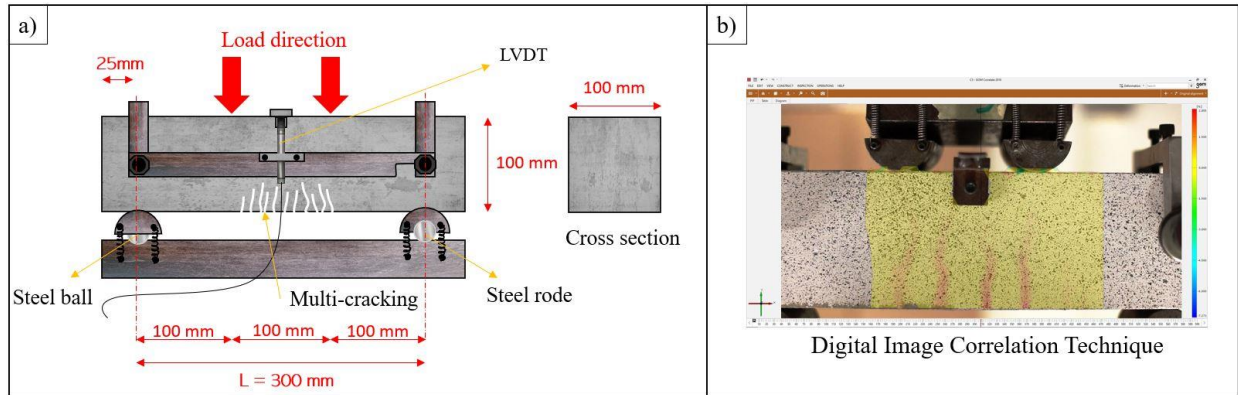


Fig. 2. Four-point bending test, a) setup and dimensions, and b) DIC technique used in the test to detect cracks and measure the crack widths

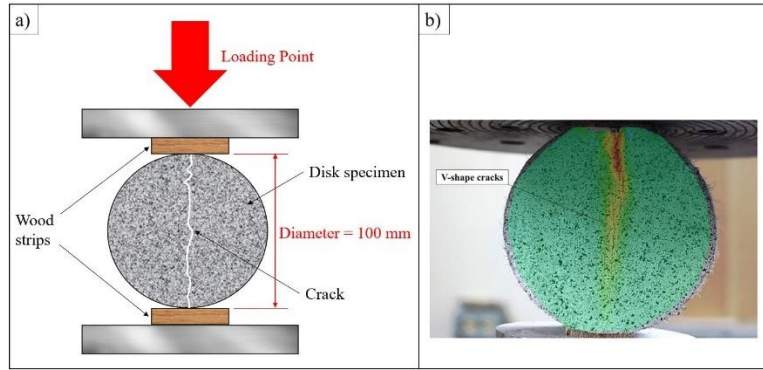


Fig. 3. Split tensile testing, a) test setup details, and b) V-shape cracks monitored via DIC

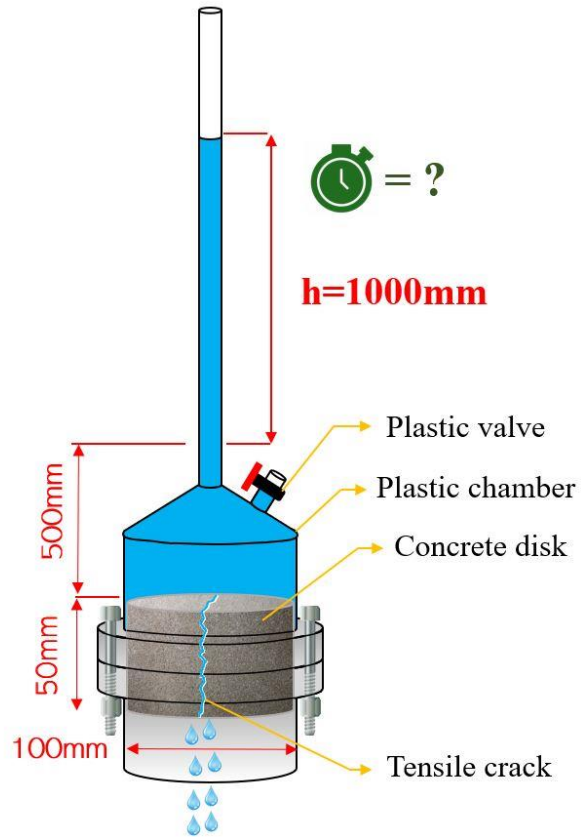


Fig. 4. Water permeability test setup

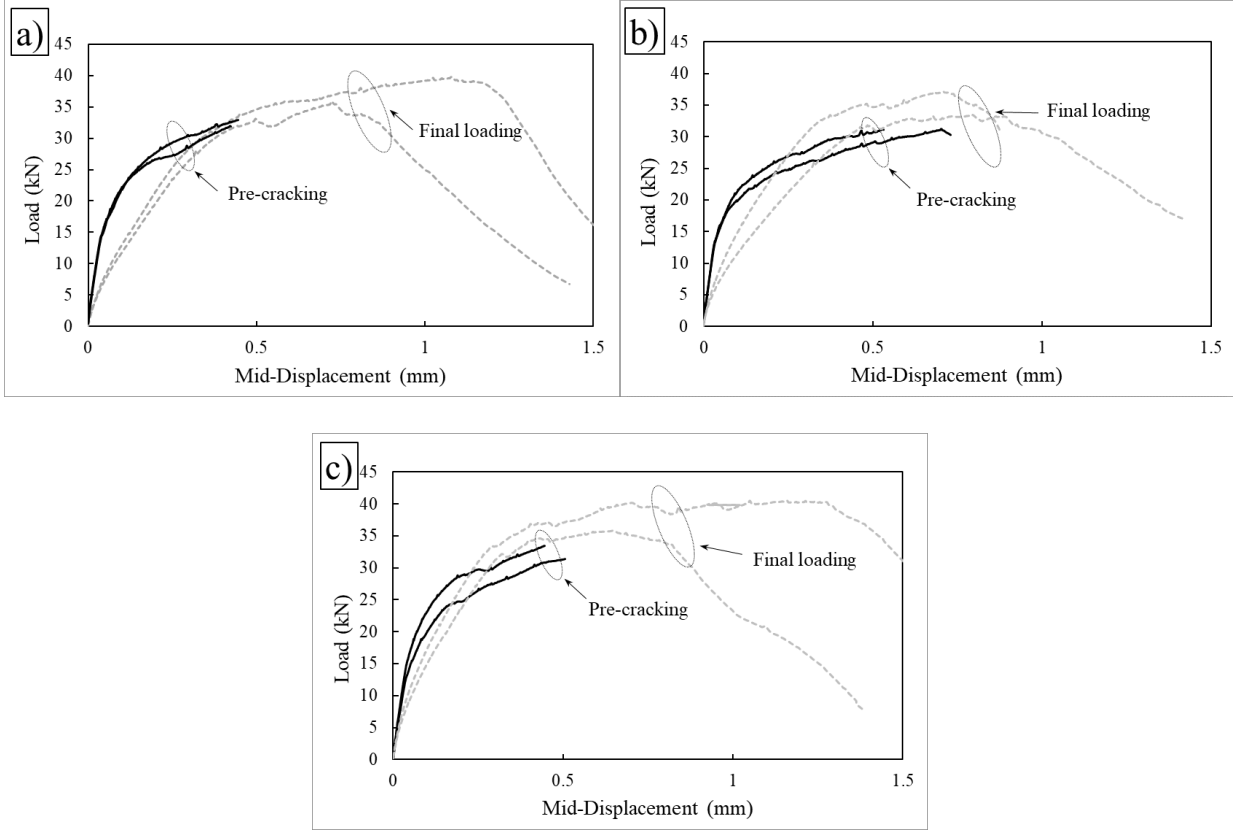


Fig. 5. Load vs. Midspan deflection of pre-cracking and final loading for different exposure conditions; a) ambient air, b) tap water and c) seawater

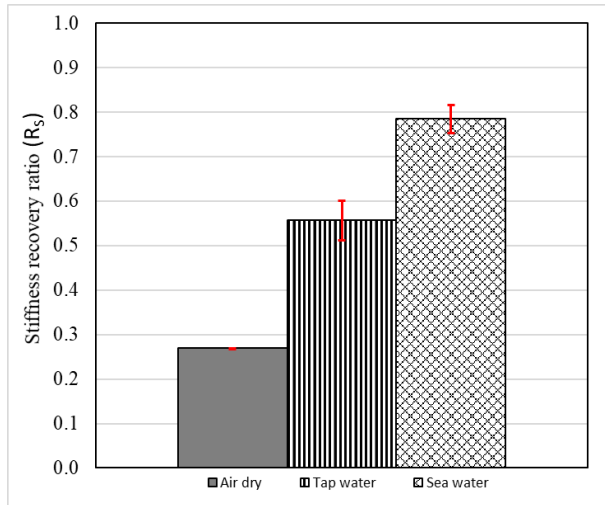


Fig. 6. Stiffness recovery ratio (R_S) of specimen groups exposed to different exposure conditions

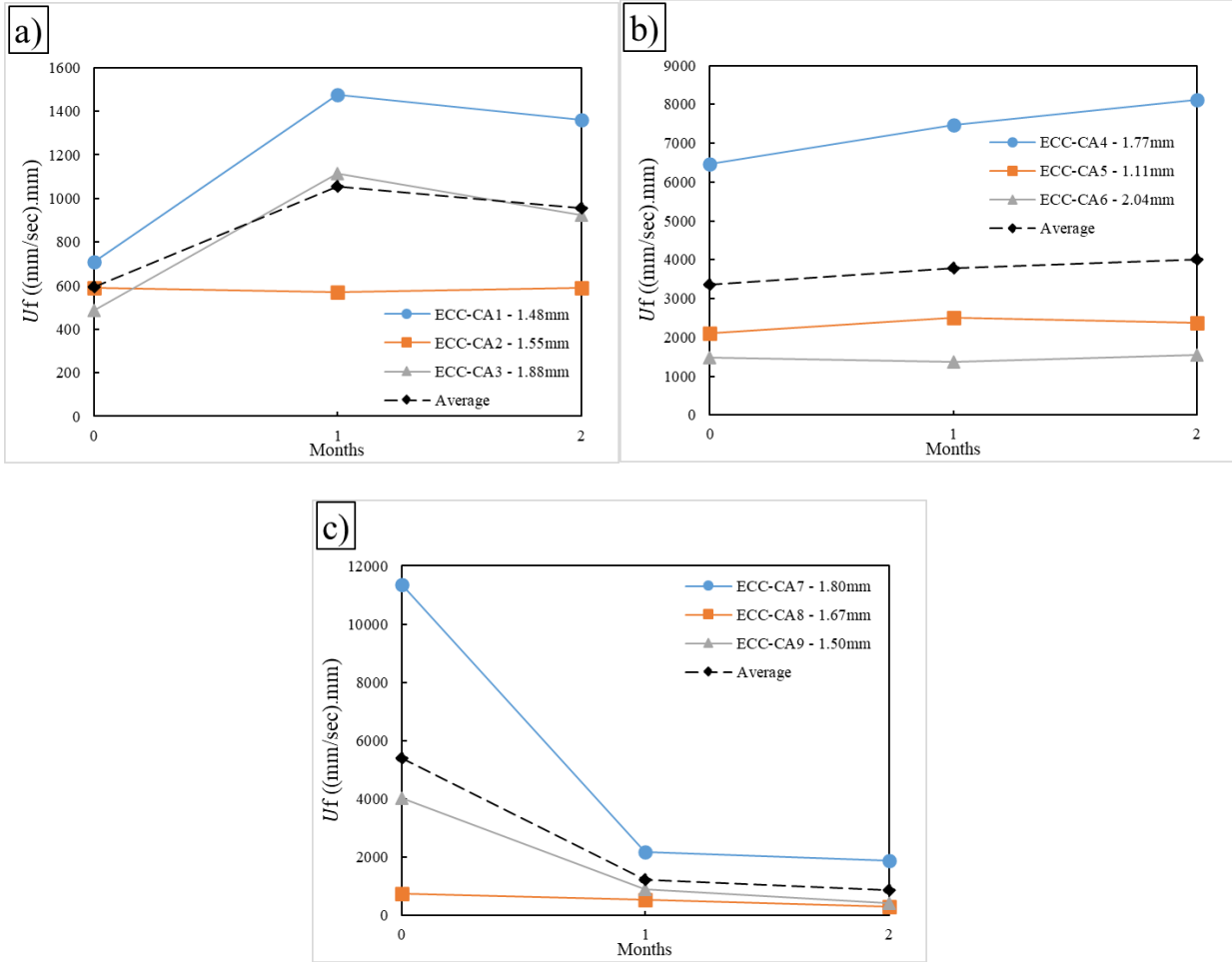


Fig. 7. Velocity factor (U_f) vs. curing time for ECC-CA specimens exposed to different exposure conditions; a) ambient air, b) tap water, and c) seawater

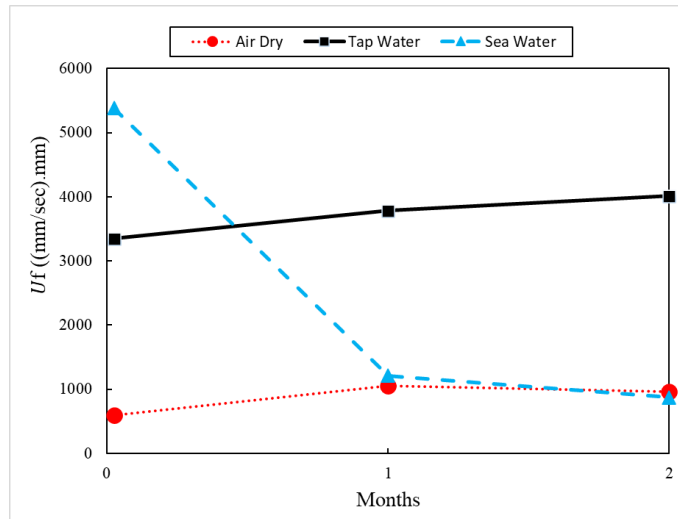


Fig. 8. Average Water Permeability (WP) results for ECC-CA specimens

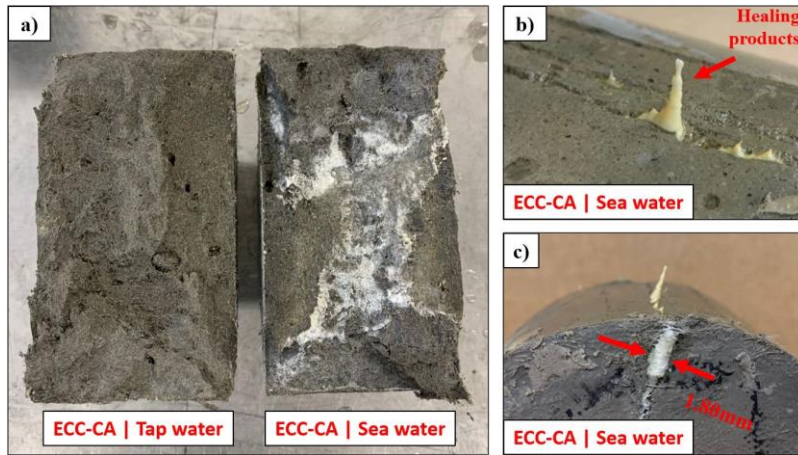


Fig. 9 ECC-CA disk specimens: a) opened up after the final water permeability test (WP3) to observe product formation inside cracks, b) healing products leaching out from the cracks and, c) 1.80mm crack filled with white precipitates

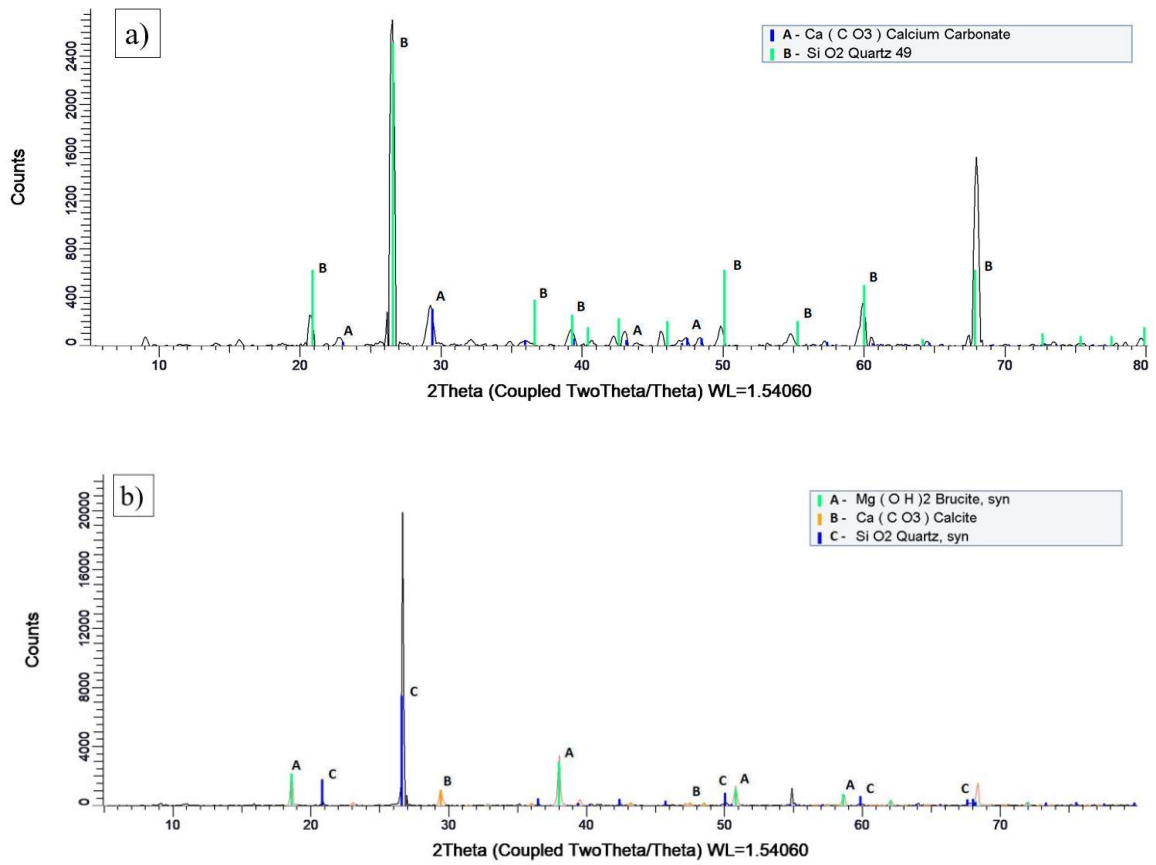


Fig. 10. XRD analysis of ECC-CA specimens exposed to a) tap water and b) seawater condition